An improved cluster dynamics model for hydrogen retention in tungsten

Article *in* International Journal of Modern Physics C · July 2012

DOI: 10.1142/S0129183112500428

CITATIONS
12

READS
84

5 authors, including:

Yonggang Li
Hefei Institute of Physical Sciences, Chinese Academy of Scie…
55 PUBLICATIONS **870** CITATIONS

SEE PROFILE

Wanghuai Zhou
Hubei University of Automotive Technology
34 PUBLICATIONS **419** CITATIONS

SEE PROFILE

Zuoyu Zeng
The University of Hong Kong
123 PUBLICATIONS **2,073** CITATIONS

SEE PROFILE

International Journal of Modern Physics C
Vol. 23, No. 6 (2012) 1250042 (12 pages)

DOI: 10.1142/S0129183112500428

World Scientific
www.worldscientific.com

AN IMPROVED CLUSTER DYNAMICS MODEL FOR HYDROGEN RETENTION IN TUNGSTEN

R. H. NING, Y. G. LI, W. H. ZHOU and Z. ZENG*

Key Laboratory for Materials Physics
Institute of Solid State Physics
Chinese Academy of Sciences
Hefei 230031, P. R. China
**zzeng@theory.issp.ac.cn*

X. JU

Department of Physics
University of Science and Technology Beijing
Beijing 100083, P. R. China

Received 29 March 2012
Accepted 25 April 2012
Published 18 June 2012

An improved cluster dynamics model has been developed for studying the behaviors of hydrogen retention in tungsten under hydrogen ions irradiation. In addition to different types of objects, adopting up-to-date parameters and complex reaction processes, we newly introduce ion-induced and natural defects into our model. This improved model programmed in IRadMat2 could describe very well the depth distributions and the amounts of hydrogen retained in tungsten under different radiation conditions. The calculated results agree with the experimental ones much better than the previous model, especially for the depth-distribution of D retained in W, which imply that this model is applicable to the evolution of defects especially for low energy high flux ions irradiated on plasma-facing materials.

Keywords: Cluster dynamics model; hydrogen retention in tungsten; ions irradiation; ion-induced and natural defect.

PACS Nos.: 02.60.Cb, 61.80.Az, 61.72.Cc, 61.72.J-.

1. Introduction

Tungsten (W) is the most promising candidate armor material for the ITER divertor and perhaps the whole first wall in the future reactors due to its good thermal properties and low sputtering erosion yield. As a plasma-facing material (PFM), W is subjected to intensive fluxes of energetic hydrogen isotope (H, D and T) and helium (He) as well as 14.1 MeV neutrons from the D-T fusion reaction.[1] Ions bombardment will produce radiation-induced defects and changes in microstructure, hence, physical

and mechanical properties.[2,3] Moreover, hydrogen isotope ions injected into W would be deeply trapped by lattice defects such as vacancies and dislocation loops formed by themselves or neutron irradiation,[4] which can further affect the fuel efficiency. Thus, issues arising from the interaction of H and tungsten are important for the design and operation of fusion devices. So far, however, the mechanism of H trapping and diffusion in W is not well understood. In order to assess the retention mechanisms, many experimental researches have been done and obtained series of results in the depth profiles and the amounts of ions retained in W etc. in recent years in ion beam and linear plasma devices.[1,5–13] However, all of the behaviors of H retention in W are related to the underlying microscopic mechanisms of defects diffusion and accumulation, unfortunately, cannot be obtained directly through experiments.

Meanwhile, the corresponding theoretical studies have also been performed using a multi-scale modeling from atomistic to continuum approaches.[14,15] Particularly, for the long-term kinetic evolution of defects, kinetic Monte Carlo (KMC)[16,17] and cluster dynamics (CD) model[4,18–20] are commonly used. On one hand, KMC model can account for the spatial and temporal correlations, but it is limited to small volumes ($\sim \mu$m), low irradiation dose (typically much less than 1 dpa) and small time scales. Becquart *et al.* have developed an object KMC model based on the *ab initio* parametrizations[16,17] to investigate the microstructural evolution of irradiated W with He, but the model cannot be applied to the case of long-range scale diffusion due to its lower efficiency. On the other hand, in spite of excluding of the stochastic effects/spatial correlations caused by the random nature of the cascade initiation, the CD model based on the mean-field rate theory can explore the evolution of defects over large space scale (intermediate-length) and over large time scales ($\sim \mu$s to years) that close to those achieved experimentally, which predict the same behavior as KMC models at least at low temperature,[21] for irradiation conditions that produce a high density of defects and for materials that have a relative high density of fixed sinks.[22] Using a simple model based on rate theory, Xu *et al.* have investigated the effects of T/He on the microstructure evolution in W during T/He and neutron irradiations.[4,18] Perhaps, more reliable parameters or more reasonable reaction mechanisms of defects should be addressed to obtain credible results. In order to obtain more reliable results of He retention in W and compare with the experiments, we have developed the CD model and investigated He retention in W during He and neutron irradiations,[19,20] where the calculated results are good agree with the experiments. However, for the case of H, the behaviors/mechanisms are quite different from He. Henriksson *et al.* shown the significant different behaviors of interstitial H and He atoms in W and explained the different bubble-formation depth of H from He as observed in the experiment.[23] Therefore, in order to investigate the H retention in W and obtain more reliable results, we should improved our previous model by considering the new features of H in W.

Thus, the aim of this work is to improve our previous CD model and further to correctly describe the behaviors of H retention in W. The present results are compared with the previous ones and the difference of H retention in W from He is

demonstrated. The new model enable us to improve the understanding of the behaviors of H retention in W.

2. Theoretical Model

Based on the framework of our CD model of He diffusion and accumulation in W,[19,20] by considering the different behaviors between H from He in W and the new features of low energy high flux H implantation, we have newly improved it by taking account of different types of objects, ion-induced defects and natural defects, adopting up-to-date parameters and complex reaction processes as well as the diffusion processes of mobile defects in a long-range space scale.

2.1. *Master equations*

The CD model used here can provide information about the roles of different migration and reaction mechanisms, as well as the diffusion processes along depth for different defects. Several assumptions are employed as following:

(1) The basic types of defects included in the model are self-interstitial atoms (SIAs, I), vacancies (V), hydrogen atoms (H) and the formed complex clusters (I_n; HI; and H_mV, where m, n is the number of defects in a loop/cluster) by binary reactions. In addition, other inherent sinks like dislocation lines (L) and vacancies are also included.
(2) Only SIAs (I), di-interstitials (I_2), vacancies (V) and hydrogen atoms (H) are considered to be mobile for simplification, while all other defect clusters are considered to be immobile.
(3) Maximal number of hydrogen atoms absorbed by a vacancy is eight according to the first principles calculations.[24]
(4) The formation of vacancy clusters and hydrogen-vacancy clusters (H_mV_n, $n > 1$) is neglected for simplification owing to the very low mobility of vacancies on the present conditions mentioned here.

The evolution of mobile defects are described in a set of one-dimensional spatial diffusion-reaction equations by taking into account their diffusion and possible reactions with other defects, while immobile clusters are described by the master equations. So, rate equations of interstitials, vacancies, hydrogen, hydrogen-interstitial and hydrogen-vacancy clusters can be expressed, respectively, as

$$\begin{aligned}\frac{\partial C_I}{\partial t} &= G_{I/V} + D_I\nabla^2 C_I - k^+_{I+V}(C_I C_V - C_I^{\mathrm{eq}} C_V^{\mathrm{eq}}) + k^+_{V+I_2} C_V C_{I_2} \\ &\quad - 2(\alpha_1^+ C_I^2 - \alpha_2^- C_{I_2}) - \sum_{n\geq 2}^{N_I} (\alpha_n^+ C_I C_{I_n} - \alpha_{n+1}^- C_{I_{n+1}}) \\ &\quad - (k^+_{H+I} C_H C_I - k^-_{HI} C_{HI}) - \sum_{m=1}^{M_H} k^+_{H_mV+I} C_I C_{H_mV} - L_I, \end{aligned} \tag{1}$$

$$\frac{\partial C_{I_2}}{\partial t} = D_{I_2}\nabla^2 C_{I_2} + (\alpha_1^+ C_I^2 - \alpha_2^- C_{I_2}) - 2(\beta_2^+ C_{I_2}^2 - \beta_4^- C_{I_4}) + k_{I_3+V}^+ C_{I_3} C_V - (\alpha_2^+ C_{I_2} C_I - \alpha_3^- C_{I_3}) - \sum_{n\geq 3}^{N_I} (\beta_n^+ C_{I_2} C_{I_n} - \beta_{n+2}^- C_{I_{n+2}}) - k_{V+I_2}^+ C_{I_2} C_V - L_{I_2}, \quad (2)$$

$$\frac{\partial C_V}{\partial t} = G_{I/V} + D_V\nabla^2 C_V - k_{I+V}^+ (C_I C_V - C_I^{\text{eq}} C_V^{\text{eq}}) - k_{I_2+V}^+ C_V C_{I_2} - \sum_{n\geq 3}^{N_I} (k_{I_n+V}^+ C_V C_{I_n} - k_{I_{n-1}-V}^- C_{I_{n-1}}) - (k_{H+V}^+ C_V C_H - k_{HV}^- C_{HV}) - k_{HI+V}^+ C_V C_{HI} - L_V, \quad (3)$$

$$\frac{\partial C_H}{\partial t} = G_H + D_H\nabla^2 C_H - (k_{H+I}^+ C_H C_I - k_{HI}^- C_{HI}) - (k_{H+V}^+ C_H C_V - k_{HV}^- C_{HV}) + \sum_{m=1}^{M_H} m k_{H_mV+I}^+ C_{H_mV} C_I - \sum_{m=1}^{M_H-1} (\mu V_m^+ C_H C_{H_mV} - \mu V_{m+1}^- C_{H_{m+1}V}) - L_H, \quad (4)$$

$$\left.\frac{\partial C_{I_n}}{\partial t}\right|_{3\leq n\leq N_I} = -(\alpha_n^+ C_I C_{I_n} - \alpha_{n+1}^- C_{I_{n+1}}) + (\alpha_{n-1}^+ C_I C_{I_{n-1}} - \alpha_n^- C_{I_n}) - (\beta_n^+ C_{I_2} C_{I_n} - \beta_{n+2}^- C_{I_{n+2}}) + (\beta_{n-2}^+ C_{I_2} C_{I_{n-2}} - \beta_n^- C_{I_n}) + (k_{I_{n+1}+V}^+ C_V C_{I_{n+1}} - k_{I_n-V}^- C_{I_n}) - (k_{I_n+V}^+ C_V C_{I_n} - k_{I_{n-1}-V}^- C_{I_{n-1}}), \quad (5)$$

$$\frac{\partial C_{HI}}{\partial t} = k_{HI}^+ C_H C_I - k_{HI}^- C_{HI} - k_{HI+V}^+ C_{HI} C_V, \quad (6)$$

$$\left.\frac{\partial C_{H_mV}}{\partial t}\right|_{1\leq m\leq M_H} = -k_{H_mV+I}^+ C_I C_{H_mV} + (k_{HV}^+ C_D C_V - k_{HV}^- C_{HV}) - (\mu V_m^+ C_H C_{H_mV} - \mu V_{m+1}^- C_{H_{m+1}V}) + (\mu V_{m-1}^+ C_H C_{H_{m-1}V} - \mu V_m^- C_{H_mV}), \quad (7)$$

where, $C_\theta^{\text{eq}}(\theta = I, V)$ are the concentrations of SIAs and vacancies at thermodynamical equilibrium, and N_I, M_H are the maximum size of interstitial loops and H atoms in H_mV complexes, respectively. Here, all equations (Eqs. (1)–(7)) are solved for a set of depth points of N_Z.

2.2. *Rate coefficients*

The rate coefficients describe the physical production rates and the rates of capture and emission of point defects by defect clusters as listed in Table 1. These

Table 1. Reaction types and the corresponding rate coefficients.

Reaction types	Rate coefficients
$I + V \rightleftharpoons 0$;	$k^+_{I+V},\ G_{I/V}$
$I + I_n \rightleftharpoons I_{n+1}$;	$\alpha^+_n,\ \alpha^-_{n+1}$
$I + H \rightleftharpoons HI$;	$k^+_{H+I},\ k^-_{HI}$
$I + H_mV \rightarrow mH$;	$k^+_{H_mV+I}$
$I_2 + I_n \rightleftharpoons I_{n+2}$;	$\beta^+_n,\ \beta^-_{n+2}$
$I_2 + V \rightarrow I$;	$k^+_{V+I_2}$
$V + I_n \rightleftharpoons I_{n-1}$;	$k^+_{I_n+V},\ k^-_{I_{n-1}-V}$
$V + H \rightleftharpoons HV$;	$k^+_{H+V},\ k^-_{HV}$
$V + HI \rightarrow H$;	k^+_{HI+V}
$H + H_mV \rightleftharpoons H_{m+1}V$;	$\mu V^+_m,\ \mu V^-_{m+1}$
$I + L \rightarrow LI$;	L_I
$I_2 + L \rightarrow LI_2$;	L_{I_2}
$V + L \rightarrow LV$;	L_V
$H + L \rightarrow LH$;	L_H

processes include the production and recombination of $I - V$ point defects and the reactions of $I_n - \theta|_{\theta=I,I_2,V}$, $V - \theta|_{\theta=I,I_2,H}$, $H - \theta|_{\theta=I,V}$, $H_mV - \theta|_{\theta=I,H}$, $HI - V$ and $L - \theta|_{\theta=I,I_2,V,H}$. The rate distribution of H near surface is estimated by TRIM-code.[25] The fundamental details of the rate coefficients are described in Refs. 19 and 20.

2.3. *Ion-induced defects*

Series of experimental researches have reported that high flux and low energy of D plasma irradiation on W can produce defects in the near surface.[26,27] Lindig *et al.* have investigated the high flux ($10^{22}\,D\,\mathrm{m^{-2}s^{-1}}$) and low energy (38 eV) of D plasma irradiated polycrystalline tungsten and reported that Cracks and large cavities were observed beneath the surface.[26] Alimov *et al.* have measured its depth distribution of D in W used the nuclear reaction analysis (NRA) method and found a D concentration peak in the near surface.[27] Ogorodnikova *et al.* pointed out that it is a nonclassical behavior of H in W, which cannot be explained by the mechanism of diffusion and trapping alone.[9] In fact, microscopic damage of W such as vacancies, interstitials and dislocation loops can be formed during high flux and low energy hydrogen implantation. When the incident flux is higher than the rate of H diffusion out of the implantation range, all traps will be filled with H and reach a local supersaturation near the surface due to the low solubility of H in W. Then one more H atom will result in tensions and stresses, which can produce ion-induced defects (interstitials, vacancies and voids etc.).[9] In our model, only Frenkel pairs are introduced as ion-induced defects for simplification.

The increase of the traps density Φ with fluence can be written in analogy to spontaneous recombination of defects in metals,[28]

$$d\Phi/dt = (1 - r)I_0\psi(x)\eta(1 - \Phi/\Phi_m), \tag{8}$$

where I_0 is the incident flux, r is the reflection coefficient, $\psi(x)$ is the depth distribution of ion-induced defects, η is the rate of the defect creation and Φ_m is the maximal defect concentration. Then the time-dependence of the trap density is given by,

$$\Phi(x,t) = \Phi_m\{1 - \exp[-(1-r)I_0\psi(x)\eta t/\Phi_m]\}, \tag{9}$$

where $\psi(x)$ is set as a Gaussian distribution for simplification.

2.4. *Numerical method*

The evolution of cluster size is then obtained through numerical resolution of large number partial differential equations (PDEs). However, the interstitial loops considered here contain a large number of SIAs, which would exceed the current capability of computers. In order to extend this limit and increase the computation efficiency, for larger size interstitial loops, the discrete master equation is usually transformed into a continuous Fokker−Plank type equation by Taylor series expansion up to second-order terms. Details of the treatment are described in Refs. 19 and 20.

The PDEs are transformed approximately to conservative finite difference equations on the nonuniform mesh by using central finite differencing, i.e. the set of ordinary differential equations (ODEs). Here, the system of ODEs is solved by using *lsoda* subroutine packages,[29] which is well known as a fast solver for ODEs based on the explicit predictor−corrector method with an automatic switch for stable and nonstable problems. In practice, the parameters are set as $n \sim$ hundreds, $M_H \sim$ several and $N_Z \sim$ tenths in general, by considering their respective precipitate size mentioned here. Thus the total number of the ODEs is estimated typically in the order of $\sim 10^3$ here. All the above formulas are programmed as IRadMat2, which is efficient enough that no more than several hours are necessary for the most time-consuming input condition when using a modern personal computer.

3. Results and Discussion

To simulate the experimental results as well as to make the results more reliable, we carefully choose parameters by considering the published values from experiments and *ab initio*/MD calculations, which are given in Table 2. Here, the capillary law approximation[19] is used to obtain the binding energies of mobile point defects (I, I_2) with different types of large loops (I_n). The binding energies of H atom with H_mV for clusters up to size 8 are obtained by *ab initio* calculations as described in Ref. 24. In order to show the improvements of the model, we take the case of deuterium (D) retention in W for example and investigate the behaviors of hydrogen isotope in W.

Figure 1 shows the depth distributions of D retained in W single crystal under 200 eV D^+ irradiation with a flux of 2×10^{18} D^+ $\mathrm{m^{-2}s^{-1}}$ up to a fluence of

Table 2. Parameters used in the case of D atoms irradiated on W.

	Symbol	Value	Refs.
H beam intensity	I_H	$10^{18} \sim 10^{22}\,\mathrm{m^{-2}s^{-1}}$	Ref. 30
Temperature	T	$300 \sim 700\,\mathrm{K}$	
Point defect creation rate	$G_{I/V}$	$10^{-6}\,\mathrm{dpa\,s^{-1}}$	Ref. 18
Lattice parameter	a_0	3.1652 Å	Ref. 31
H radius	r_H	0.53 Å	
Burgers vector	b	2.74 Å	Ref. 31
Recombination radius	r_{IV}	4.65 Å	Estimated
Maximal defect concentration	Φ_m	$3.15 \times 10^{27}\,\mathrm{m^{-3}}$	Ref. 9
The rate of defect creation	η	1×10^{-3}	Ref. 9
Interstitial pre-exponential factor	D_{I_o}	$1.0e^{-8}\,\mathrm{m^{-2}s^{-1}}$	Refs. 32, 33
Vacancy pre-exponential factor	D_{V_o}	$1.0e^{-8}\,\mathrm{m^{-2}s^{-1}}$	Refs. 32, 33
D pre-exponential factor	D_{H_o}	$4.1e^{-7}\,\mathrm{m^{-2}s^{-1}}$	Ref. 1
Bias factor of interstitial loops	Z_I	1.2	Ref. 18
Formation energy of SIA	E_I^f	9.466 eV	Ref. 34
Formation energy of Vacancy	E_V^f	3.80 eV	Ref. 34
Formation energy of H	E_H^f	2.45 eV	Ref. 35
Migration energy of SIA	E_I^m	0.013 eV	Ref. 36
Migration energy of Vacancy	E_V^m	1.66 eV	Ref. 37
Migration energy of H	E_H^m	0.39 eV	Ref. 38
Binding energy of I_2	$E_{I_2}^b$	2.12 eV	Ref. 17
Binding energy of $H - I$	E_{H-I}^b	0.33 eV	Ref. 16
Binding energy of HV	E_{HV}^b	1.18 eV	Ref. 24

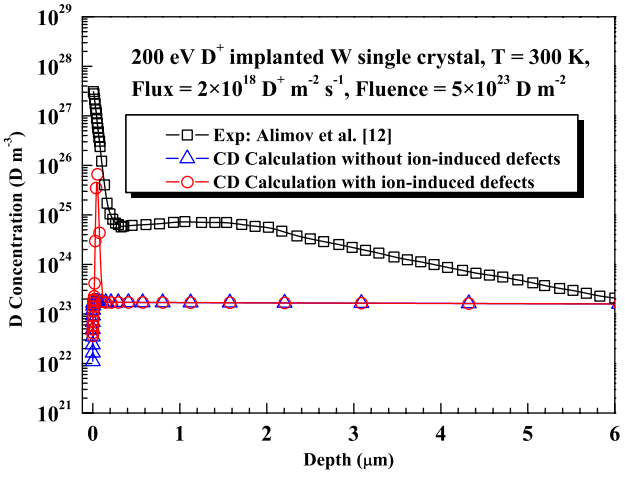

Fig. 1. (Color online) Calculated and experimental[12] depth profiles of D in W single crystal under D^+ implantation with energy of 200 eV and a flux of 2×10^{18} D^+ $\mathrm{m^{-2}s^{-1}}$ up to a fluence of 5×10^{23} D $\mathrm{m^{-2}}$ at 300 K.

5×10^{23} $D\,m^{-2}$ at 300 K. The experimental result[12] shows a D concentration peak appears in the near surface region, which is a nonclassical behavior of low energy H irradiation on W, cannot be explained by the mechanism of diffusion and trapping alone.[9] In fact, ion-induced traps should be formed in this region leading to a D concentration peak. In our previous CD model, SRIM code[25] is used to estimate the rate distribution of ion-induced defects near the surface. However, according to TRIM calculations, 200 eV D^+ cannot produce Frenkel pairs in W due to the small energy transfer, so that no D concentration peak exists as shown in Fig. 1. By introducing ion-induced defects in the present model, a D concentration peak also appears in the near surface region as experiment. The lower peak of the concentration obtained from the calculation than that from experiment can be affected by many factors. On one hand, the manufacture and pre-treatment of W and measurement errors in experiments can significantly affect the experimental results of D retention in W.[5,7,9–13] On the other hand, several approximations introduced in the present model, that is, excluding the formations of V_n and D_mV_n $(n > 1)$ clusters and neglecting the adsorption of D by ion-induced dislocation loops, would also cause the deviation. In fact, voids and bubbles could be induced during D^+ implantation in the near surface, which can trap a fraction of D in the form of D_mV_n.[26] However, owing to the very low mobility of vacancies on the condition mentioned here, they are also neglected in our model.[4] Moreover, both the previous and present model is only considering the adsorption of D by dislocation lines in the bulk, thus, the calculated results do not describe the experimental depth profile much well. Further improvements of the model are required as discussed below.

As shown in Fig. 2, the depth distributions of D in polycrystalline W are given under 200 eV D^+ irradiation with different implantation fluxes, fluences and irradiation temperatures. The experimental results by Alimov *et al.*[12,13] show the features of D retention in polycrystalline W in several respects, i.e. a peak in the near surface layer (0−0.2 μm), a decrease in the sub-surface layer (0.2−3 μm) as well as a steady state in the bulk (at least after 3 μm). The previous calculations consider the natural defects (dislocations and grain boundaries (GBs)) just as the inherent sinks of mobile defects ($I,\ I_2,\ V,\ He,\ H$) with the uniform and infinite adsorption. In the case of low flux of He implantation, these approximations are reasonable as shown in Refs. 19 and 20. However, for the case of high flux of D implantation, previous model cannot describe the experimental depth at all as shown in Fig. 2, which is mainly due to the different trapping mechanisms of H and He atoms in W[23]: On the one hand, He can trap with other He atoms to form bubble seeds, while the H−H interaction in the W lattice is repulsive at short H−H distances, preventing self-trapping. On the other hand, vacancies or vacancy clusters can trap He much more than H.

In fact, both single and polycrystalline W have natural defects not only the dislocation lines but also vacancies, interstitials, impurities etc. For polycrystalline W, GB is another factor that significantly affect the behaviors of D retention in W. Zhou *et al.*[39] have investigated the trapping mechanisms of H by a tungsten GB based on the first-principle method and found that the GB can hold no more than 2 H

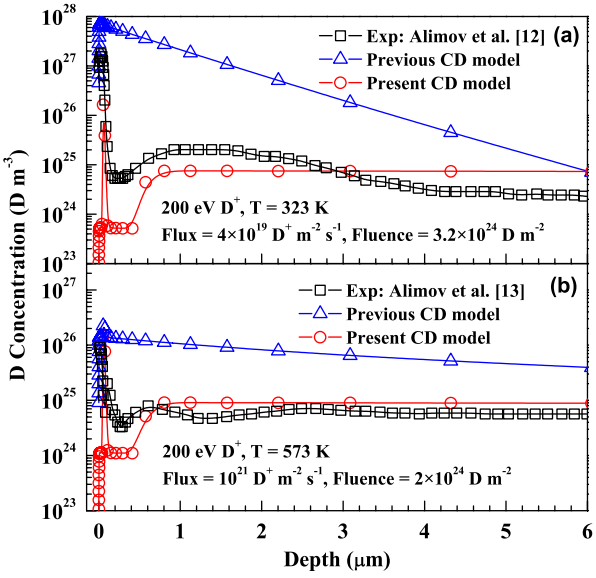

Fig. 2. (Color online) Calculated and experimental[12,13] depth profiles of D in polycrystalline W under D^+ implantation with energy of 200 eV and (a) a flux of 4×10^{19} D^+ $\mathrm{m^{-2}s^{-1}}$ up to a fluence of 3.2×10^{24} D $\mathrm{m^{-2}}$ at 323 K; (b) a flux of 10^{21} D^+ $\mathrm{m^{-2}s^{-1}}$ up to a fluence of 2×10^{24} D $\mathrm{m^{-2}}$ at 573 K.

atoms because the isosurface of optimal charge density almost disappears with the second H atom in. It is the reason why the approximation of GBs as a type of inherent sinks for mobile D does not describe the experimental results in our previous model. Taking into account the lower vacancy formation energy in the GB as compared with the bulk, Zhou *et al.* proposed that the experimentally observed H bubble formation in the W GB should be *via* a vacancy trapping mechanism. Furthermore, it is also necessary to consider the intrinsic vacancies in our model, thus, we just include dislocations and vacancies as the natural defects in W for simplification as Ogorodnikova *et al.* did in Ref. 9.

By considering ion-induced defects and natural defects in polycrystalline W, we applied our model to investigate the behaviors of D retention in polycrystalline W as shown in Fig. 2. Good agreements between experiment and modeling are obtained with different calculation conditions,[12,13] which implies that the mechanisms of vacancy trapping significantly affect the behaviors of D retention in polycrystalline W. However, experimental result shows a D concentration platform in the range of $(1-3\,\mu\mathrm{m})$ which is not seen in our calculation as shown in Fig. 2(a). With the ions implantation, ion-induced vacancies are formed around the implantation area and cause a D concentration peak near surface, while the interstitials migrate much deeper into the bulk due to its high diffusivity and form dislocation loops in this region, we propose that the D concentration platform is mainly contributed by the adsorption of dislocation loops. When the temperature increased to 573 K, the

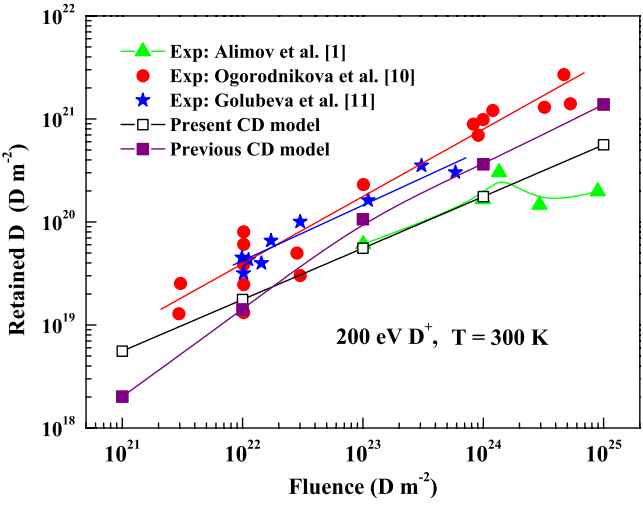

Fig. 3. (Color online) Calculated and experimental[1,10,11] fluence dependence of the amounts of retained D in W irradiated with 200 eV D^+ at 300 K.

platform disappears as shown in Fig. 2(b) due to the lower binding energy between H and dislocation loops.

Implantation of hydrogen isotope into W PFMs leads to much concerns about ions inventory after long-term plasma exposure. The amounts of ions retained in W are usually measured by nuclear reaction analysis (NRA) and thermal desorption spectroscopy (TDS).[1] However, theoretical investigation about that is still insufficiency. Based on our previous and present CD model, we calculate the amounts of D retained in W with different ion fluences. The results are comparable with the experimental as shown in Fig. 3. The results obtained by the present model follow a linear increase along the increasing fluence like different experimental results while the results from previous model have a little difference. The amount of D retained in W for both of the models have a similar trend with the increasing fluence at high incident fluence, while the trend calculated by the previous model increases faster than the present model at low incident fluence, which is mainly due to the poor approximation of that the infinite adsorption rate of D by GBs increases with the increasing fluence. Moreover, Tian *et al.*[7] used TDS method to investigate the fluence dependence of D retention in W with different types of tungsten specimens, ion energies and irradiation temperatures and found a saturation trend for incident fluences above 2×10^{24} D m^{-2} under 200 eV D^+ irradiation on Rembar foil at 300 K. For the case of high incident fluence, cracks and pores etc. may occur during ion implantation, diffusion may be impeded in the near-surface preventing trapping sites from deep in the bulk. We concern this is a most possible explanation for the saturation trend at 300 K. However, a further study is still needed to look insight the influence of high incident fluence.

4. Conclusions

To investigate the behaviors of H retention in W, an improved CD model has been developed based on a previous CD model which could simulate the behaviors of He retention in W with satisfaction. Due to the different mechanisms of diffusion and accumulation between H and He in W, we improve the CD model in the present work by involving different types of objects, ion-induced defects and natural defects, adopting up-to-date parameters and complex reaction processes as well as considering the diffusion and accumulation processes along depth, which are implanted in the code IRadMat2. The depth distributions of H in W with different fluxes, fluences and temperatures are investigated as well as the fluence dependence of the amount of H retained in W. The results from the improved model are comparable with the experiments much well. It concludes that: Firstly, low energy H implantation can also cause ion-induced defects which trapped lots of H atoms and formed a H concentration peak in the near-surface. Secondly, ion-induced SIAs migrate to the subsurface layer and recombine with the inherent vacancies and D_mV clusters, leading to the H concentration decreases in this region. Finally, the amount of H retained in W follows a linear increase along the increasing fluence when the fluence ranged from 10^{21} to 10^{25} D m^{-2}.

Acknowledgments

This work was supported by special Funds for Major State Basic Research Project of China (973) under Grant Nos. 2008CB717802 and 2012CB933702, Knowledge Innovation Program of Chinese Academy of Sciences under Grant No. KJCX2-YW-N35, National Science Foundation of China under Grant Nos. 11005124 and 11174284 and of Anhui Province No. 1208085QA05, and Director Grants of CASHIPS. The calculations were performed in Center for Computational Science of CASHIPS and on the ScGrid of Supercomputing Center, Computer Network Information Center of Chinese Academy of Sciences.

References

1. C. H. Skinner *et al.*, *Fusion Sci. Technol.* **54**, 891 (2008).
2. S. L. Dudarev and J.-L. Boutard *et al.*, *J. Nucl. Mater.* **386**, 1 (2009).
3. A. Manhard, K. Schmid, M. Balden and W. Jacob, *J. Nucl. Mater.* **415**, S632 (2011).
4. Q. Xu, K. Sato and T. Yoshiie, *J. Nucl. Mater.* **390**, 663 (2009).
5. J. P. Roszell, A. A. Haasz and J. W. Davis, *J. Nucl. Mater.* **415**, S641 (2011).
6. R. A. Causey, D. F. Cowgill and R. Doerner *et al.*, *J. Nucl. Mater.* **415**, S672 (2011).
7. Z. Tian, J. W. Davis and A. A. Haasz, *J. Nucl. Mater.* **399**, 101 (2010).
8. O. V. Ogorodnikova, *J. Nucl. Mater.* **390**, 651 (2009).
9. O. V. Ogorodnikova, J. Roth and M. Mayer, *J. Appl. Phys.* **103**, 034902 (2008).
10. O. V. Ogorodnikova, J. Roth and M. Mayer, *J. Nucl. Mater.* **373**, 254 (2008).
11. A. V. Golubeva, M. Mayer, J. Roth, V. A. Kurnaev and O. V. Ogorodnikova, *J. Nucl. Mater.* **363**, 893 (2007).
12. V. Kh. Alimov, J. Roth and M. Mayer, *J. Nucl. Mater.* **337**, 619 (2005).

13. V. Kh. Alimov and J. Roth, *Phys. Scr.* **T128**, 6 (2007).
14. M. Samaras, M. Victoria and W. Hoffelner, *Nucl. Eng. Tech.* **41**, 1 (2009).
15. C. S. Becquart and C. Domain, *Met. Mater. Trans. A* **42A**, 852 (2011).
16. C. S. Becquart and C. Domain, *J. Nucl. Mater.* **385**, 223 (2009).
17. C. S. Becquart, C. Domain, U. Sarkar, A. DeBacker and M. Hou, *J. Nucl. Mater.* **403**, 75 (2010).
18. Q. Xu, N. Yoshida and T. Yoshiie, *J. Nucl. Mater.* **367**, 806 (2007).
19. Y. G. Li, W. H. Zhou, R. H. Ning, L. F. Huang, Z. Zeng and X. Ju, *Commu. Comput. Phys.* **11**, 1547 (2011).
20. Y. G. Li, W. H. Zhou, L. F. Huang, Z. Zeng and X. Ju, *J. Nucl. Mater.* in press, DOI: 10.1016/j.jnucmat.2011.12.015 (2011).
21. C. J. Ortiz and M. J. Catural, *Phys. Rev. B* **75**, 184101 (2007).
22. R. E. Stoller, S. I. Golubov, C. Domain and C. S. Becquart, *J. Nucl. Mater.* **382**, 77 (2008).
23. K. O. E. Henriksson, K. Nordlund, A. Krasheninnikov and J. Keinonen, *Appl. Phys. Lett.* **87**, 163113 (2005).
24. Y.-L. Liu, Y. Zhang, H.-B. Zhou, G.-H. Lu, F. Liu and G.-N. Luo, *Phys. Rev. B* **79**, 172103 (2009).
25. J. P. Biersack and L. G. Haggmark, *Nucl. Instrum. Methods* **174**, 257 (1980), TRIM/SRIM website, http://www.srim.org.
26. S. Lindig, M. Balden, V. Kh. Alimov, T. Yamanishi, W. M. Shu and J. Roth, *Phys. Scr.* **T138**, 014040 (2009).
27. V. Kh. Alimov, W. M. Shu, J. Roth, K. Sugiyama, S. Lindig, M. Balden, K. Isobe and T. Yamanishi, *Phys. Scr.* **T138**, 014048 (2009).
28. O. V. Ogorodnikova, J. Roth and M. Mayer, *J. Nucl. Mater.* **313**, 469 (2003).
29. L. R. Petzold, *SIAM J. Sci. Stat. Comput.* **4**, 136 (1983).
30. W. M. Shu, G.-N. Luo and T. Yamanishi, *J. Nucl. Mater.* **367**, 1463 (2007).
31. M. P. Surh, J. B. Sturgeon and W. G. Wolfer, *J. Nucl. Mater.* **378**, 86 (2008).
32. N. M. Ghoniem and S. Sharafat, *J. Nucl. Mater.* **92**, 121 (1980).
33. M. P. Surh, J. B. Sturgeon and W. G. Wolfer, *J. Nucl. Mater.* **325**, 44 (2007).
34. P. A. T. Olsson, *J. Nucl. Mater.* **47**, 135 (2009).
35. F. Christien and A. Barbu, *J. Nucl. Mater.* **324**, 90 (2004).
36. A. H. Duparc, C. Moingeon, N. S. de Grande and A. Barbu, *J. Nucl. Mater.* **302**, 143 (2002).
37. F. Christien and A. Barbu, *J. Nucl. Mater.* **393**, 153 (2009).
38. P. M. Derlet, D. Nguyen-Manh and S. L. Dudarev, *Phys. Rev. B* **76**, 054107 (2007).
39. H.-B. Zhou, Y.-L. Liu, S. Jin, Y. Zhang, G.-N. Luo and G.-H. Lu, *Nucl. Fusion* **50**, 025016 (2010).